Author Manuscript
Author Manuscript
Author Manuscript
Author Manuscript

HHS Public Access
Author manuscript
J Infrared Millim Terahertz Waves. Author manuscript; available in PMC 2021 July 20.

Published in final edited form as:
J Infrared Millim Terahertz Waves. 2021 May ; 42: 547–556. doi:10.1007/s10762-021-00769-8.

Study of the Effect of Reflections on High-Power, 110 GHz Pulsed Gyrotron Operation

J. Genoud[1], **J. F. Picard**[1], **S. C. Schaub**[2], **S. K. Jawla**[1], **M. A. Shapiro**[1], **R. J. Temkin**[1]

[1]Massachusetts Institute of Technology (MIT), Plasma Science and Fusion Center (PSFC), Cambridge, MA 02139 USA,

[2]Air Force Research Laboratory, Albuquerque, NM, 87117, USA

Abstract

The effect of reflection is studied experimentally and theoretically on a high-power 110 GHz gyrotron operating in the $TE_{22,6}$ mode in 3 μs pulses at 96 kV, 40 A. The experimental setup allows variation of the reflected power from 0 to 33 % over a range of gyrotron operating conditions. The phase of the reflection is varied by translating the reflector along the axis. Operating at a higher efficiency point, at 4:40 T with 940 kW of output power, reflected power exceeding 11% causes a switch from operation in the $TE_{22,6}$ to simultaneous operation in the $TE_{22,6}$ and $TE_{21,6}$ modes with a large decrease of the total gyrotron output power. This switching effect is in good agreement with simulations using the MAGY code. Operating at a more stable point, 4:44 T with 580 kW of output power, when the reflection is increased, the output power remains in the $TE_{22,6}$ mode but it decreases monotonically with increasing reflection, dropping to 200 kW at 33% reflection. Furthermore, at a reflection above 22%, a power modulation at 25 to 30 MHz is observed, independent of the phase of the reflected wave. Such a modulated signal may be useful in spectroscopic and other applications.

1 Introduction

The study of the effect of rf-wave reflections is of particular interest and has been a subject of concern for at least two decades in the high-power gyrotron community [1, 2]. For high-power gyrotrons used for plasma heating for fusion applications, the reflections could stem from the output window, the transmission line between the gyrotron and the plasma, or by the first layer of the plasma itself [3]. Reflections can be favorable for gyrotron operation when they are controlled and limited, and have been shown to increase the rf output power [4, 5], lock the gyrotron oscillation frequency [6], decrease the sensitivity of the radiation frequency to variation of the magnetic field [2], extend the frequency range by exciting different axial modes [7, 8], and suppress parasitic modes [9]. However, when not controlled, even a limited amount of reflection can lead to a complete loss of oscillation by driving the gyrotron to a non-stationary or chaotic phase or into unstable operation in an undesired mode. If another mode is excited, the generated microwave power will be trapped inside the gyrotron tube because the quasi-optical output mirror assembly is designed only for the particular frequency of the operating mode. Several numerical or experimental publications have discussed the fact that such uncontrolled reflection can decrease the onset

Author Manuscript

Author Manuscript

Author Manuscript

Author Manuscript

of nonstationary oscillations [10, 11, 12], competing transverse modes [13, 14], or directly decrease the generated power [5, 15].

In that context, and in view of future high-power gyrotron development for fusion reactors, it is crucial to address and understand the effects of such reflections. Such a study is challenging on a high- power continuous gyrotron due to the amount of energy reflected back. As such, the high-power short-pulse 110 GHz gyrotron at MIT is a convenient device for this study. The generated power is about 1.5 MW, but the pulse duration is 3 μs. This considerably limits the rf-wave energy, allowing the use of a simple reflector located directly in front of the output window.

The manuscript is organized as follows: in Section 2 the gyrotron and the variable reflector setup are presented; in Section 3 the main results are discussed for two operating points; in section 4, the results from simulations are presented; and Section 5 concludes the paper.

2 Experimental setup

The MIT 1.5 MW, 110 GHz, short pulse gyrotron was built to validate the design of a long pulse gyrotron for plasma heating systems [16]. The gyrotron has since been used for several essential theoretical or experimental studies, including, in particular, after-cavity interaction [17] and startup scenario studies [18]. The modularity of the tube has allowed for the study of components relevant to high-power gyrotron for plasma heating, such as a single-stage depressed collector [19], a smooth mirror mode converter [20], and a new cavity capable of producing radiation at 110 GHz or 124 GHz [21]. It has also been used extensively for various applications, including dielectric multipactor measurements [22], gas breakdown studies [23] and is currently used as a source for testing an externally driven particle accelerator structure [24, 25]. Recently, the gyrotron has been modified by installing an internal mode converter that couples the rf to a corrugated waveguide inside the gyrotron. It has been shown that with the internal mode converter, the gyrotron performance was unchanged and a 97.5 ± 1% $HE_{1,1}$ mode content is obtained [26].

The variable reflector setup is located directly in front of the internal mode converter and output window, as can be seen in a photograph in Fig. 1 and the corresponding schematic in Fig. 2. The reflected fraction or rf power is adjusted by using the $\lambda/2$ rotating waveplate, which is made of a sapphire birefringent crystal, in conjunction with the two polarizing filters. The two polarizing filters are each composed of 5 parallel quartz plates placed at the Brewster angle in order to transmit only one specific polarization of the electromagnetic wave. The $\lambda/2$ waveplate rotates the rf-wave polarization, allowing for precise tuning of the rf-wave reflected fraction. The first polarizing filter has been added to ensure that the reflected wave entering the gyrotron has the correct linear polarization. The reflector mirror is mounted on a translation stage to vary the phase of the reflected rf-wave. The calibration of the reflection fraction with respect to the rotating waveplate angle has been done by using a Vector Network Analyzer (VNA). The reflection percentage from the setup can be tuned precisely from 3% to 33%. A beam splitter in front of the gyrotron window directs a small portion of the output power to a diode (not shown in Fig. 1) to monitor the gyrotron power on each shot.

Author Manuscript

3 Experimental Results

Figure 3 presents a mode map showing the excited modes as a function of the main magnetic field and the magnetic field at the cathode. The power reflection measurements were done at two different operating points, highlighted with the two stars in Fig. 3, and for the parameters listed in Table 1. The first point, labeled A, is a high-efficiency high-power operating point. The main magnetic field value is 4.40 T, and the rf-frequency for the operating mode $TE_{22,6}$ is 110.00 GHz. This point is close to the excitation region of the competing mode $TE_{21,6}$. The second operating point, labeled B, is a more stable operating point. The main magnetic field value is 4.44 T and the rf-frequency is 110.11 GHz.

3.1 High-efficiency point

The main result for the high-efficiency point is shown in Fig. 4, where the measured output power is reported as a function of the reflection percentage. The power slightly increases for small reflection and drops significantly for a reflection higher than 11%. Above 11% both the $TE_{22,6}$ operating mode and the $TE_{21,6}$ competing mode are excited during the pulse. Figs. 5 and 6 show the cathode voltage, beam current, and pulse measured by the rf-diode for two different reflection percentages. For a limited 3.3% reflection only the $TE_{22,6}$ mode is excited during the pulse and a typical high-power pulse trace is observed, as seen in Fig. 5. For a reflection percentage of 13.2% (Fig. 6) the $TE_{21,6}$ mode is excited during the second part of the pulse, degrading significantly the average power during the pulse. The excitation of both the $TE_{22,6}$ and $TE_{21,6}$ modes has been observed for every phase of the wave reflected. The only difference seen while varying the phase is a modest modulation of the power and of the reflection threshold above which the two modes are simultaneously excited.

3.2 Stable operating point

The results for the gyrotron output power as a function of the reflection percentage at the stable operating point are shown in Fig. 7. Unlike the high-efficiency case, only the operating mode $TE_{22,6}$ is excited, even for high reflection. The main effect is a continuous reduction of rf-power with increased reflection. For reflection lower than 21%, the mode $TE_{22,6}$ is excited and the pulse is similar to the one shown in Fig. 5. For higher reflection values, a large power modulation at 27 MHz is observed, as shown in Fig. 8 for 22% reflection. This power modulation is always observed above the reflection threshold value up to the maximum reflection allowed by the setup, namely 33%. The reflection threshold leading to this power modulation depends on the phase of the wave reflected. The frequency of the power modulation is always comprised between 25 and 30 MHz and is independent of any experimental parameters, such as the gyrotron magnetic field, the reflection percentage or the phase of the wave reflected.

The physical mechanism leading to the power modulation is not yet understood and would require further investigation. It could be caused by mode competition with the mode reflected. After the reflection, the wave goes through the mode converter in the opposite direction and ends up with the opposite rotation compared to the initial mode generated in the cavity. This effect was theoretically predicted [27] and observed recently with a high-

Author Manuscript Author Manuscript Author Manuscript Author Manuscript

power 300 GHz gyrotron [28]. However, the power modulation could also be caused by a Fabry-Perot effect between the experimental setup and the gyrotron window or by an electron beam instability.

4 Simulations

The multimode code MAGY [29] was used to simulate the effect of reflections. MAGY is a self-consistent multimode code based on a time dependent description of the electromagnetic fields that computes the beam-wave interaction in the presence of reflections. The results from the simulation for the high-efficiency operating point are shown in Fig. 9. The main simulation parameters are reported in Table 2 and are close to the experimental parameters. The transition at 11% reflection from a high-power regime with the excitation of the single operating $TE_{22,6}$ mode to the simultaneous excitation of the $TE_{22,\ 6}$ and competing $TE_{21,6}$ mode is accurately predicted numerically. The power discrepancies between the measurements and the theory are likely associated to some differences between the experimental and numerical parameters considered.

5 Conclusion

A variable reflector setup has been designed and constructed to study the effect of high reflection, up to 33%, on a high-power gyrotron. The setup has been used at two different operating points, revealing two main phenomena. For a high-efficiency operating point close to the operational regime, where 1 MW is generated, reflection higher than 11% forces the excitation of the competing $TE_{21,6}$ mode simultaneously with the $TE_{22,6}$ mode, leading to a significant decrease of the power radiated. This effect has been accurately predicted by numerical simulations with the multimode code MAGY. For a more stable operating point, the reflection leads to a power modulation of the $TE_{22,6}$ operating mode at 25 – 30 MHz. The physical mechanism leading to this modulation is not understood and has still to be investigated further. Such a high frequency power modulation of the generated wave could be used in various applications, such as for DNP-NMR spectroscopy.

Acknowledgements

This work was supported by DOE, FES grant DEFC02-93ER54186, DOE HEP grant DE-SC0015566 and by NIH NIBIB grants R01-EB001965 and R01-EB004866. The authors would like to thank Alexander Vlasov and Nikita Ryskin for helpful discussions.

References

1. Antonsen TM, Cai SY, and Nusinovich GS. Effect of window reflection on gyrotron operation. Physics of Fluids B: Plasma Physics, 4(12):4131–4139, 12 1992.
2. Bogdashov AA, Fokin AP, Glyavin M. Yu., Novozhilova Yu. V., and Sedov AS. Experimental Study of the Influence of Reflections from a Non-resonant Load on the Gyrotron Operation Regime. Journal of Infrared, Millimeter, and Terahertz Waves, 41(2):164–170, 2 2020.
3. Ram AK and Hizanidis K. Scattering of radio frequency waves by cylindrical density laments in tokamak plasmas. Physics of Plasmas, 23(2):022504, 2 2016.
4. Dammertz G, Braz O, Chopra AK, Koppenburg K, Kuntze M, Piosczyk B, and Thumm M. Recent results of the 1-MW, 140-GHz, TE/sub 22,6/-mode gyrotron. IEEE Transactions on Plasma Science, 27(2):330–339, 4 1999.

Author Manuscript Author Manuscript Author Manuscript Author Manuscript

5. Dumbrajs O, Idehara T, Watanabe S, Kimura A, Sasagawa H, Agusu L, Mitsudo S, and Piosczyk B. Reflections in gyrotrons with axial output. IEEE Transactions on Plasma Science, 32(3):899–902, 6 2004.
6. Glyavin M. Yu., Denisov GG, Kulygin ML, Mel'nikova MM, Novozhilova Yu. V., and Ryskin NM. Gyrotron Frequency Stabilization by a Weak Reflected Wave. Radiophysics and Quantum Electronics, 58(9):673–683, 2 2016.
7. Khutoryan EM, Idehara T, Melnikova MM, Ryskin NM, and Dumbrajs O. Influence of Reflections on Frequency Tunability and Mode Competition in the Second-Harmonic THz Gyrotron. Journal of Infrared, Millimeter, and Terahertz Waves, 38(7):824–837, 7 2017.
8. Melnikova MM, Rodina AA, Rozhnev AG, and Ryskin NM. Self-Consistent Simulation of the Second-Harmonic 0.4-THz Gyrotron with Delayed Reflection. In 2020 45th International Conference on Infrared, Millimeter and Terahertz Waves, Buffalo, NY, United States of America, 11 2020.
9. Melnikova MM., Grigorieva N, and Ryskin NM. Influence of reflected or external signal on gyrotron operation. In Proc. SPIE 11582, Tomsk, Russian Federation, 11 2020.
10. Airila MI, Dumbrajs O, Reinfelds A, and U. Strautiņš. Nonstationary oscillations in gyrotrons. Physics of Plasmas, 8(10):4608–4612, 9 2001.
11. Airila MI and Kall P. Effect of reflections on nonstationary gyrotron oscillations. IEEE Transactions on Microwave Theory and Techniques, 52(2):522–528, 2 2004.
12. Glyavin MY and Zapevalov VE. Reflections Influence on the Gyrotron Oscillation Regimes. International Journal of Infrared and Millimeter Waves, 19(11):1499–1511, 11 1998.
13. Gantenbein G, Borie E, Dammertz G, Kuntze M, Nickel H, Piosczyk B, and Thumm M. Experimental results and numerical simulations of a high power 140 GHz gyrotron. IEEE Transactions on Plasma Science, 22(5):861–870, 10 1994.
14. Dumbrajs O. Influence of Possible Reflections on the Operation of European ITER Gyrotrons. Journal of Infrared, Millimeter, and Terahertz Waves, 31(8):892–898, 8 2010.
15. Kharchev N, Cappa Á, Malakhov D, Martínez J, Konchekov E, Tolkachev A, Borzosekov V, Sarksyan K, and Petelin M. Influence of Controlled Reflected Power on Gyrotron Performance. Journal of Infrared, Millimeter, and Terahertz Waves, 36(12):1145–1156, 12 2015.
16. Anderson JP, Shapiro MA, Temkin RJ, Mastovsky I, and Cauffman SR. Studies of the 1.5-MW 110-GHz gyrotron experiment. IEEE Transactions on Plasma Science, 32(3):877–883, 6 2004.
17. Hidaka Y, Choi EM, Mastovsky I, Shapiro MA, Sirigiri JR, and Temkin RJ. Effects of after cavity interaction in a 1.5 MW, 110 GHz gyrotron with a depressed collector. In 2008 33rd International Conference on Infrared, Millimeter and Terahertz Waves, pages 1–2, 9 2008.
18. Tax DS, Sinitsyn OV, Guss WC, Mastovsky I, Nusinovich GS, Shapiro MA, Antonsen TM, and Temkin RJ. Mode excitation during start-Up of a 1.5 MW, 110 GHz gyrotron. In 2011 International Conference on Infrared, Millimeter, and Terahertz Waves, pages 1–2, 10 2011.
19. Choi EM, Cerfon AJ, Mastovsky I, Shapiro MA, Sirigiri JR, and Temkin RJ. Efficiency Enhancement of a 1.5-MW, 110-GHz Gyrotron with a Single-Stage Depressed Collector. Fusion Science and Technology, 52(2):334–339, 8 2007.
20. Tax DS, Choi EM, Mastovsky I, Neilson JM, Shapiro MA, Sirigiri JR, Temkin RJ, and Torrezan AC. Experimental Results on a 1.5 MW, 110 GHz Gyrotron with a Smooth Mirror Mode Converter. Journal of Infrared, Millimeter, and Terahertz Waves, 32(3):358–370, 3 2011.
21. Tax DS, Rock BY, Fox BJ, Jawla SK, Schaub SC, Shapiro MA, Temkin RJ, and Vernon RJ. Experimental Results for a Pulsed 110/124.5-GHz Megawatt Gyrotron. IEEE Transactions on Plasma Science, 42(5):1128–1134, 5 2014.
22. Schaub SC, Shapiro MA, and Temkin RJ. Measurement of Dielectric Multipactor Thresholds at 110 GHz. Physical Review Letters, 123(17):175001, 10 2019. [PubMed: 31702277]
23. Schaub SC, Hummelt JS, Guss WC, Shapiro MA, and Temkin RJ. Electron density and gas density measurements in a millimeter-wave discharge. Physics of Plasmas, 23(8):083512, 8 2016.
24. Picard JF, Schaub SC, Rosenzweig G, Stephens JC, Shapiro MA, and Temkin RJ. Laser-driven semiconductor switch for generating nanosecond pulses from a megawatt gyrotron. Applied Physics Letters, 114(16):164102, 4 2019. [PubMed: 32127718]

Author Manuscript
Author Manuscript
Author Manuscript
Author Manuscript

25. Othman MAK, Picard JF, Schaub SC, Dolgashev VA, Lewis SM, Neilson JM, Haase A, Jawla S, Spataro B, Temkin RJ, Tantawi S, and Nanni EA. Experimental demonstration of externally driven millimeter-wave particle accelerator structure. Applied Physics Letters, 117(7):073502, 8 2020.
26. Neilson JM, Ives RL, Schaub SC, Guss WC, Rosenzweig G, Temkin RJ, and Borchard P. Design and High-Power Test of an Internal Coupler to HE11 Mode in Corrugated Waveguide for High-Power Gyrotrons. IEEE Transactions on Electron Devices, 65(6):2316–2320, 6 2018.
27. Dumbrajs O, Nusinovich GS, and Piosczyk B. Reflections in gyrotrons with radial output: consequences for the ITER coaxial gyrotron. In Infrared and Millimeter Waves, Conference Digest of the 2004 Joint 29th International Conference on 2004 and 12th International Conference on Terahertz Electronics, 2004., pages 187–188, 9 2004.
28. Saito T, Melnikova MM, Ryskin NM, Tanaka S, Shinbayashi R, Yuusuke Yamaguchi, Masafumi Fukunari, and Yoshinori Tatematsu. Effect of Reflection on Mode Competition and Multi-Frequency Oscillation in a High-Power Sub-THz Gyrotron: Experimental Observation and Theoretical Analysis. Journal of Infrared, Millimeter, and Terahertz Waves, 41(6):697–710, 6 2020.
29. Botton M, Antonsen TM, Levush B, Nguyen KT, and Vlasov AN. MAGY: a time-dependent code for simulation of slow and fast microwave sources. IEEE Transactions on Plasma Science, 26(3):882–892, 6 1998.

Author Manuscript
Author Manuscript
Author Manuscript
Author Manuscript

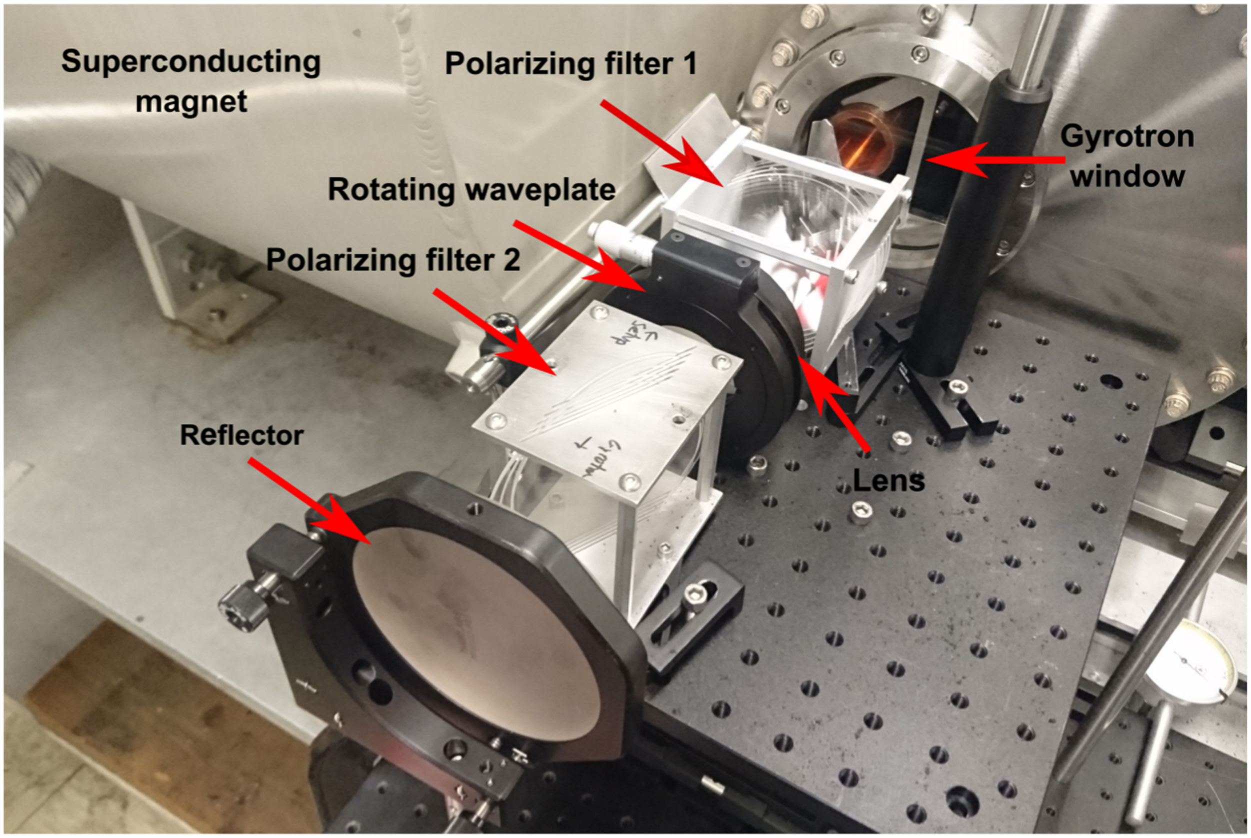

Fig. 1.
Reflection experiment setup, located directly in front of the 110 GHz gyrotron window.

Author Manuscript Author Manuscript Author Manuscript Author Manuscript

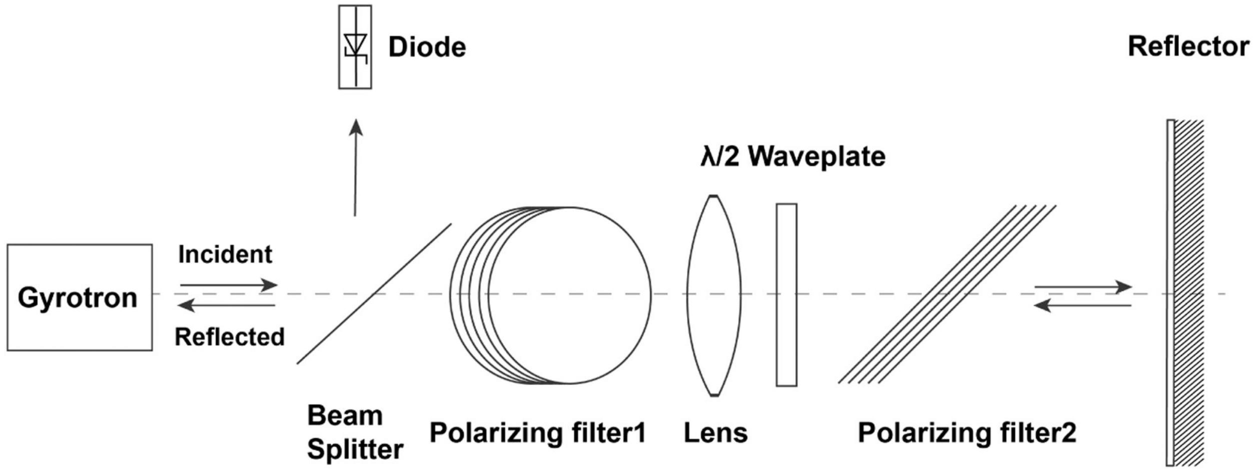

Fig. 2.
Scheme of the reflection experiment setup (view from above).

Author Manuscript
Author Manuscript
Author Manuscript
Author Manuscript

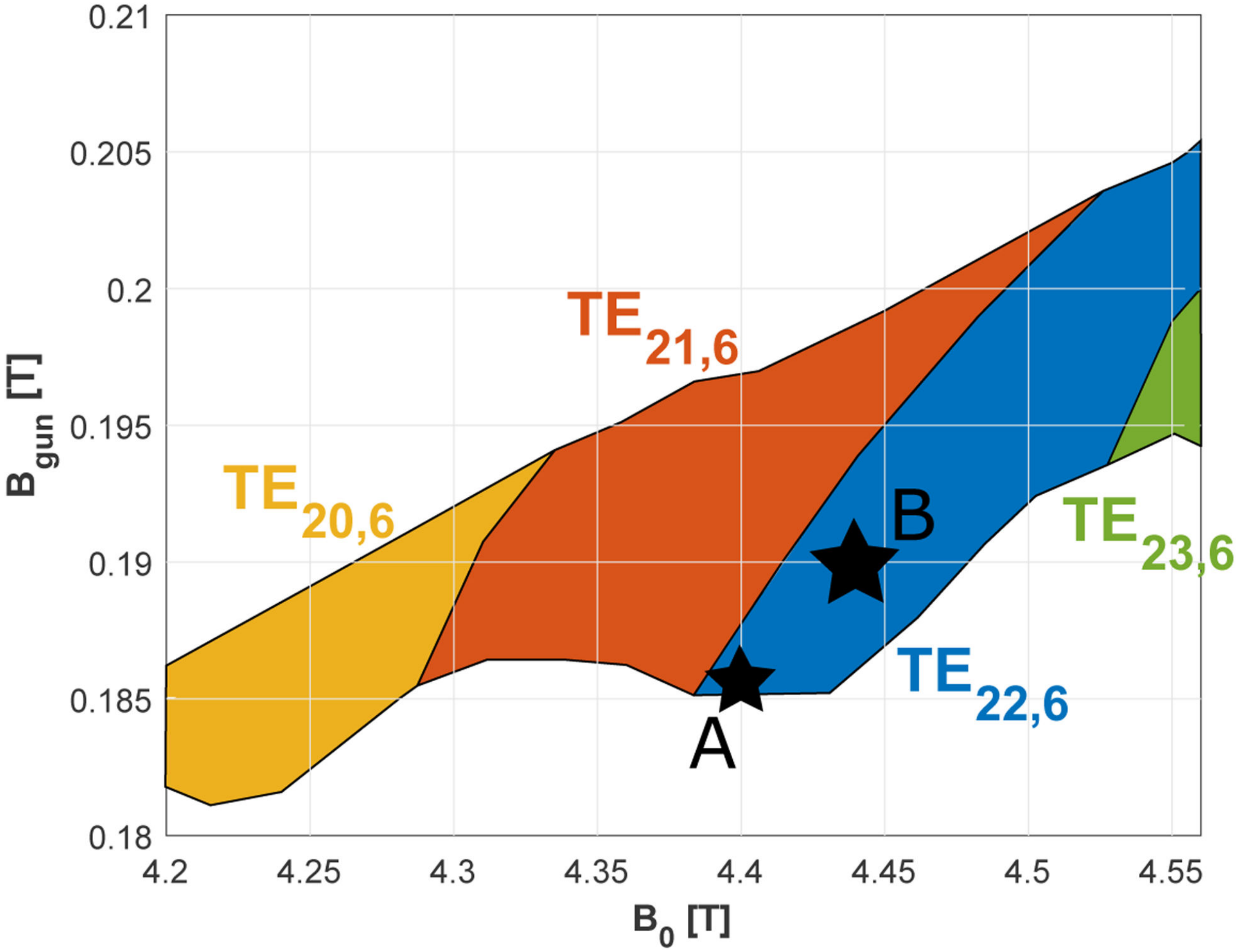

Fig. 3.

Operating mode map in the gun and main magnetic field plane. The two operating points studied are indicated with the two stars A (high-efficiency) and B (stable).

Author Manuscript
Author Manuscript
Author Manuscript
Author Manuscript

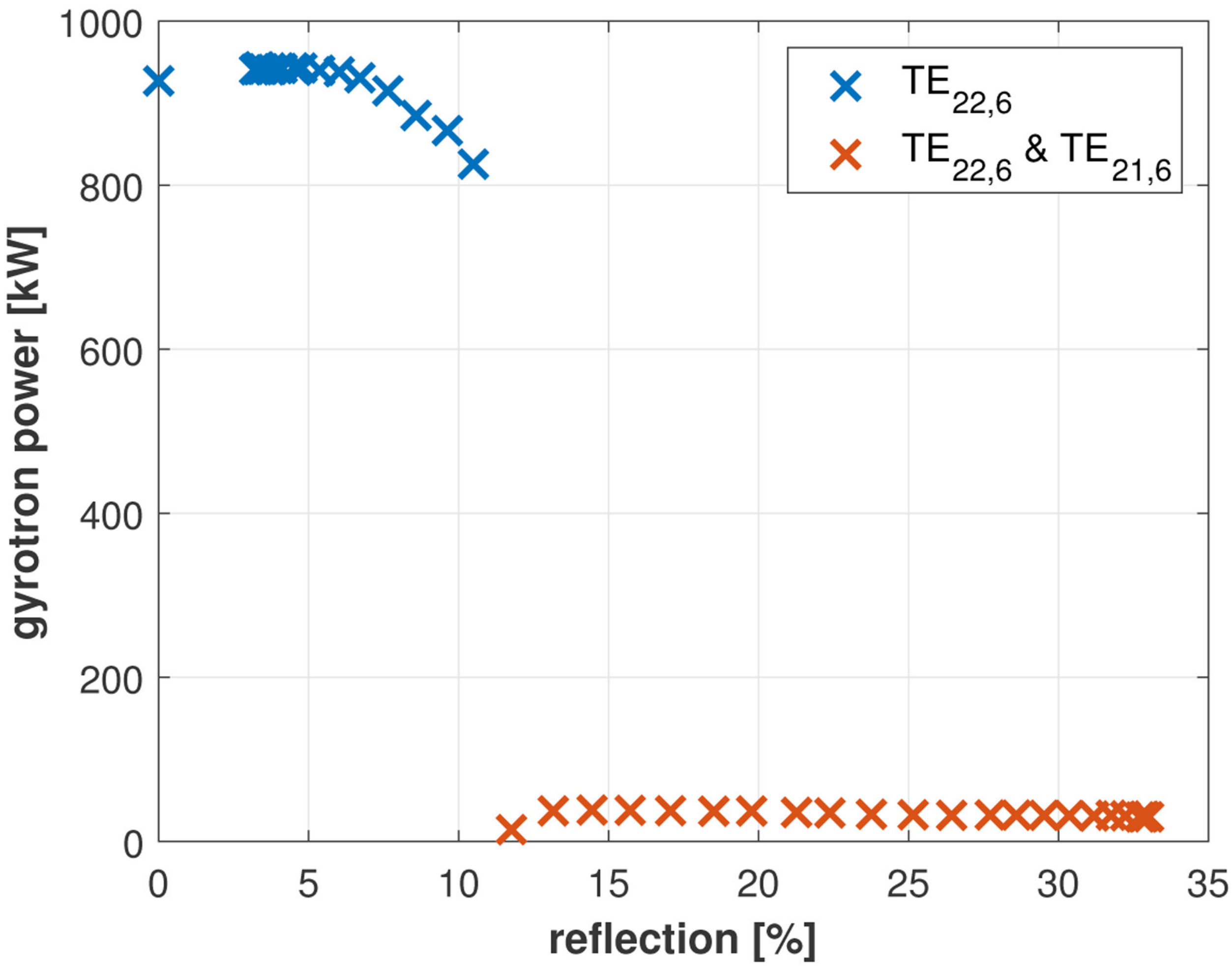

Fig. 4.
High-efficiency operating point. Gyrotron power versus reflected percentage.

Author Manuscript
Author Manuscript
Author Manuscript
Author Manuscript

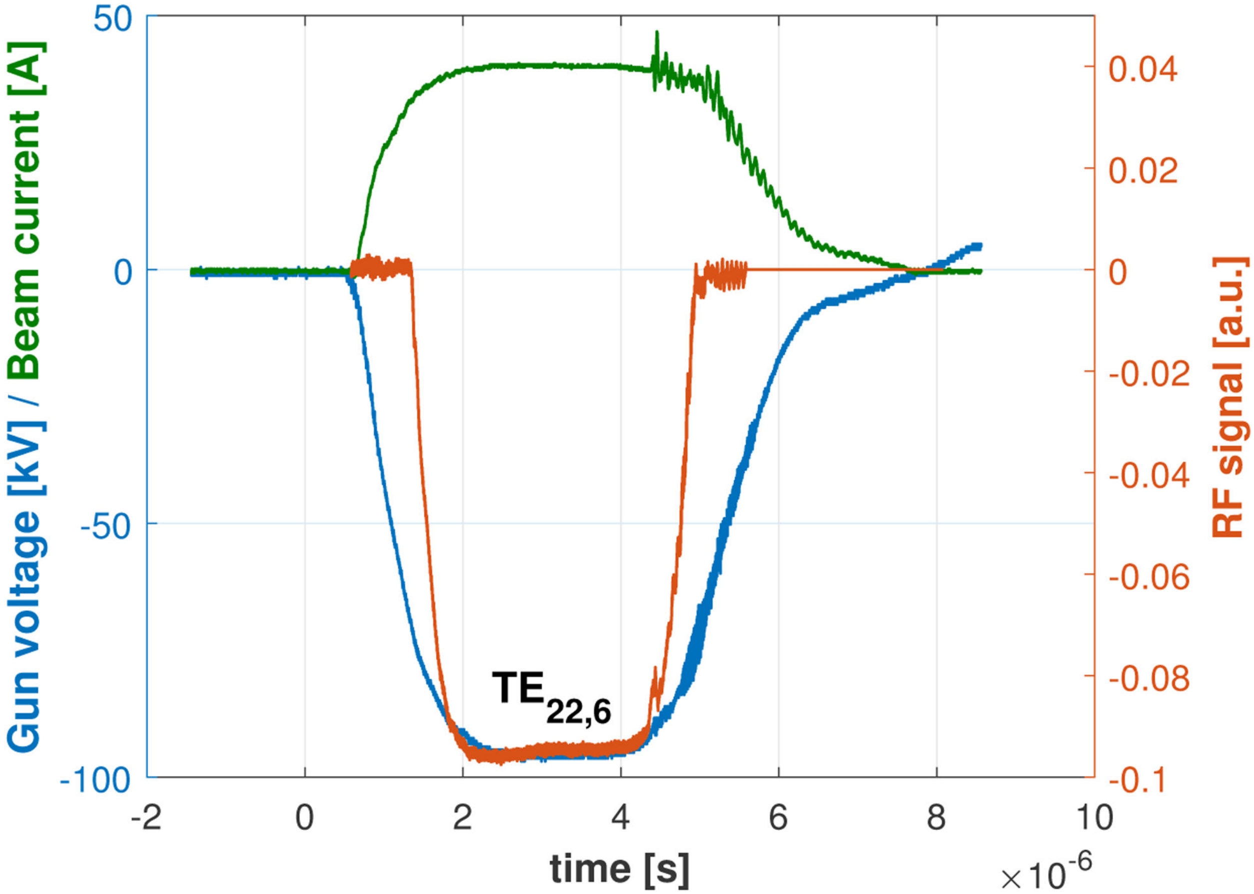

Fig. 5.

High-efficiency operating point. Time traces of the gun voltage (blue), beam current (green) and rf-signal (red) during the pulse for a percentage of reflected power of 3.3%..

Author Manuscript

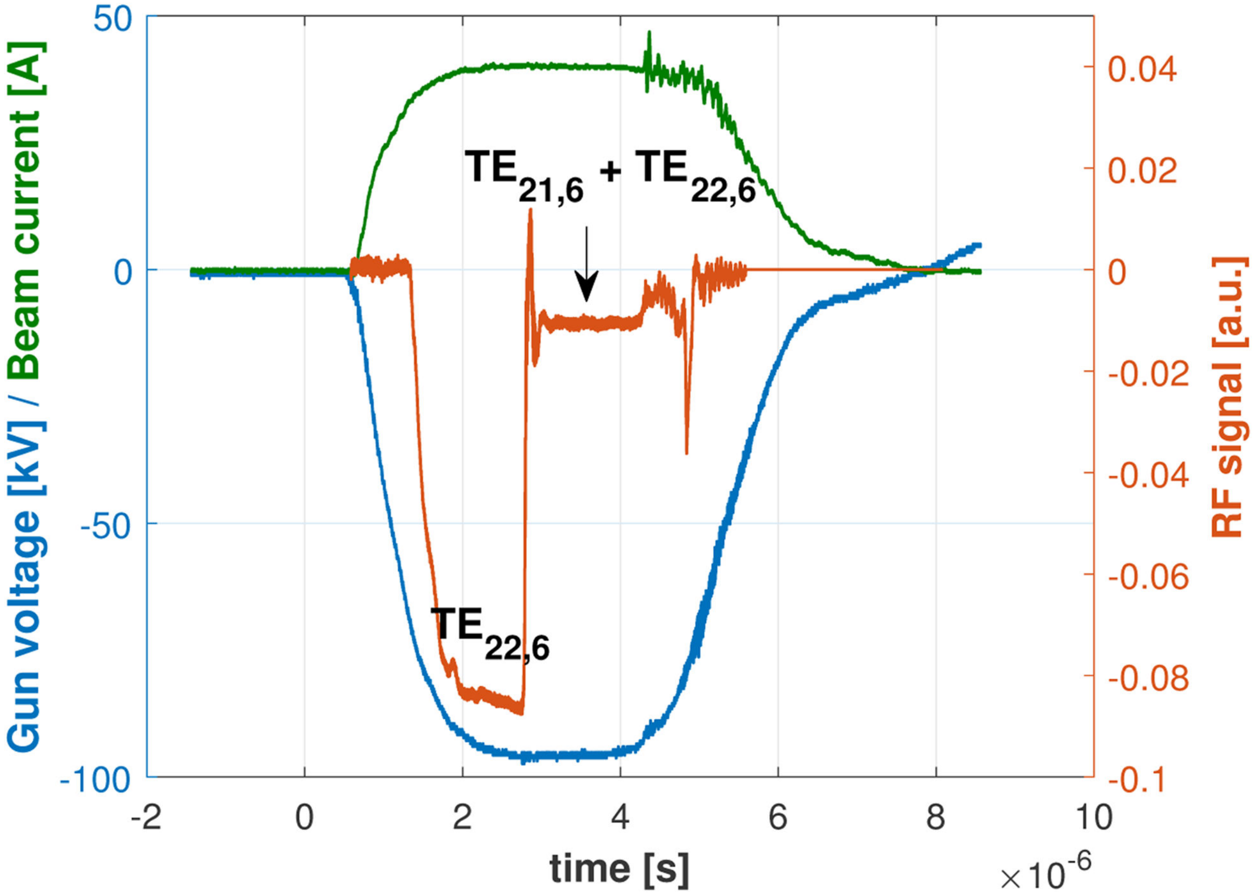

Fig. 6.

High-efficiency operating point. Time traces of the gun voltage (blue), beam current (green) and rf-signal (red) during the pulse for a percentage of reflected power of 13.2%.

Author Manuscript
Author Manuscript
Author Manuscript
Author Manuscript

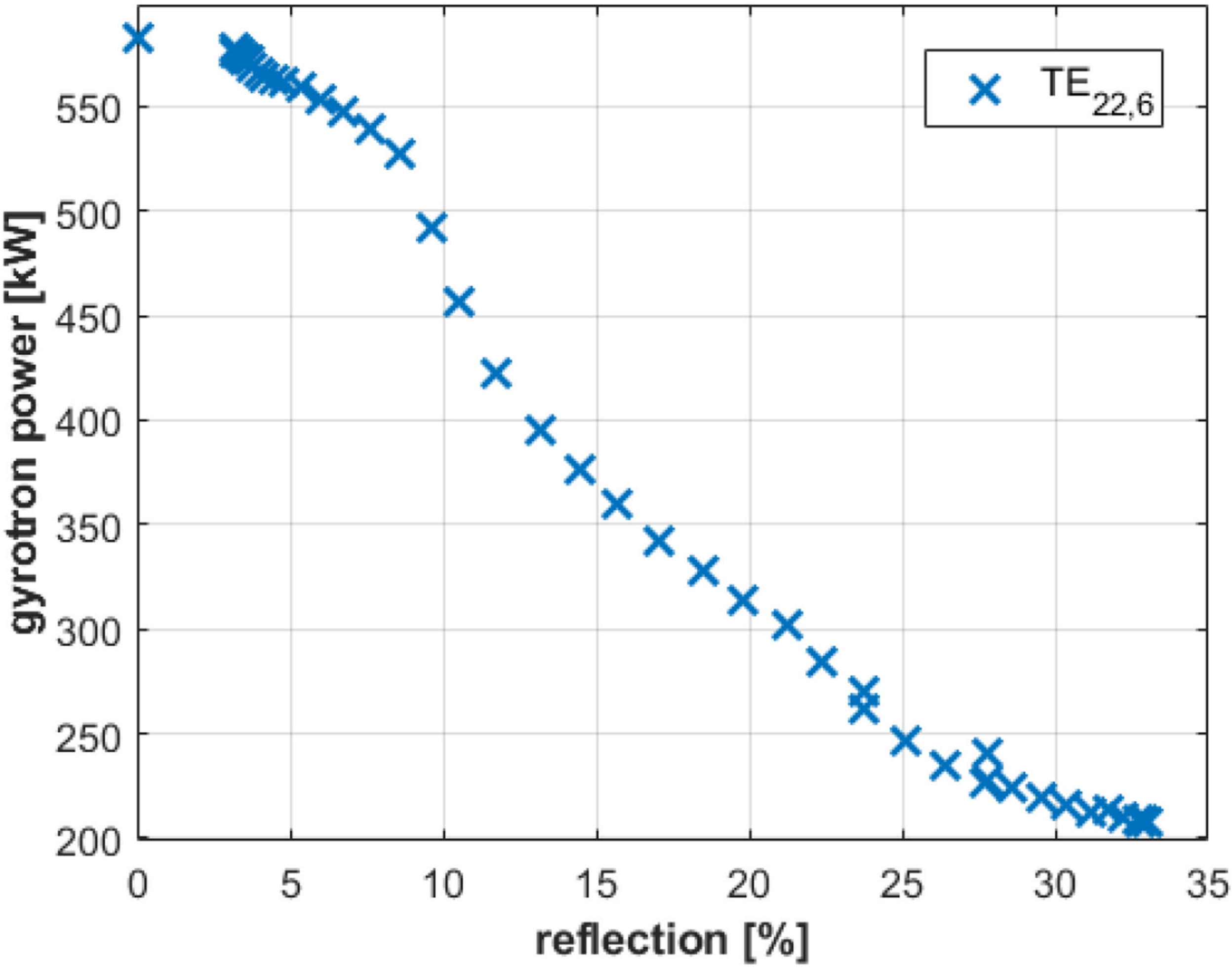

Fig. 7.
Stable operating point. Gyrotron power versus reflection percentage.

Author Manuscript
Author Manuscript
Author Manuscript
Author Manuscript

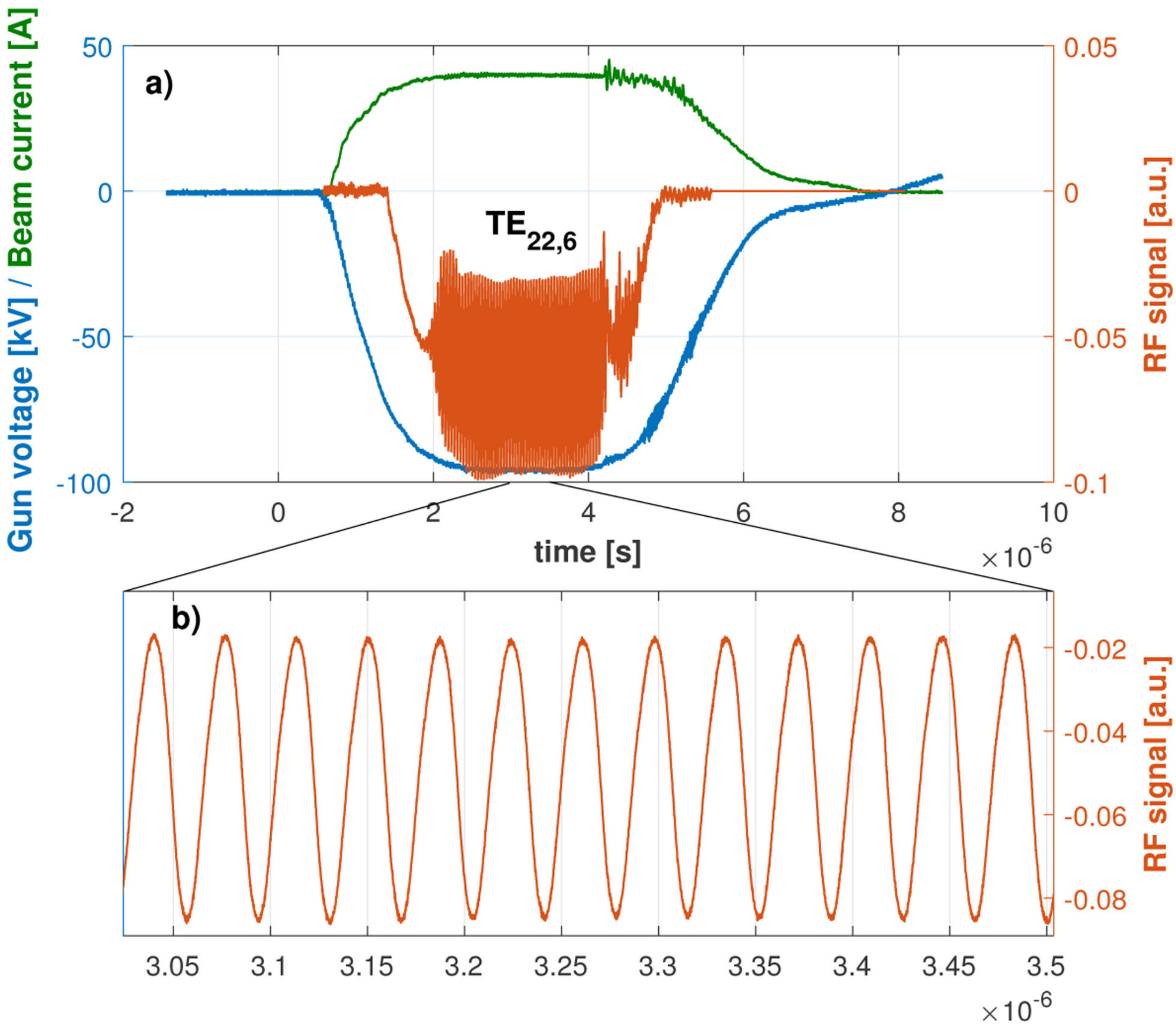

Fig. 8.

Stable operating point. a)Time traces of the gun voltage (blue), beam current (green) and rf-signal (red) during the pulse for a reflection percentage of 22.4%. b) Detail of the rf-signal pulse during the power modulation.

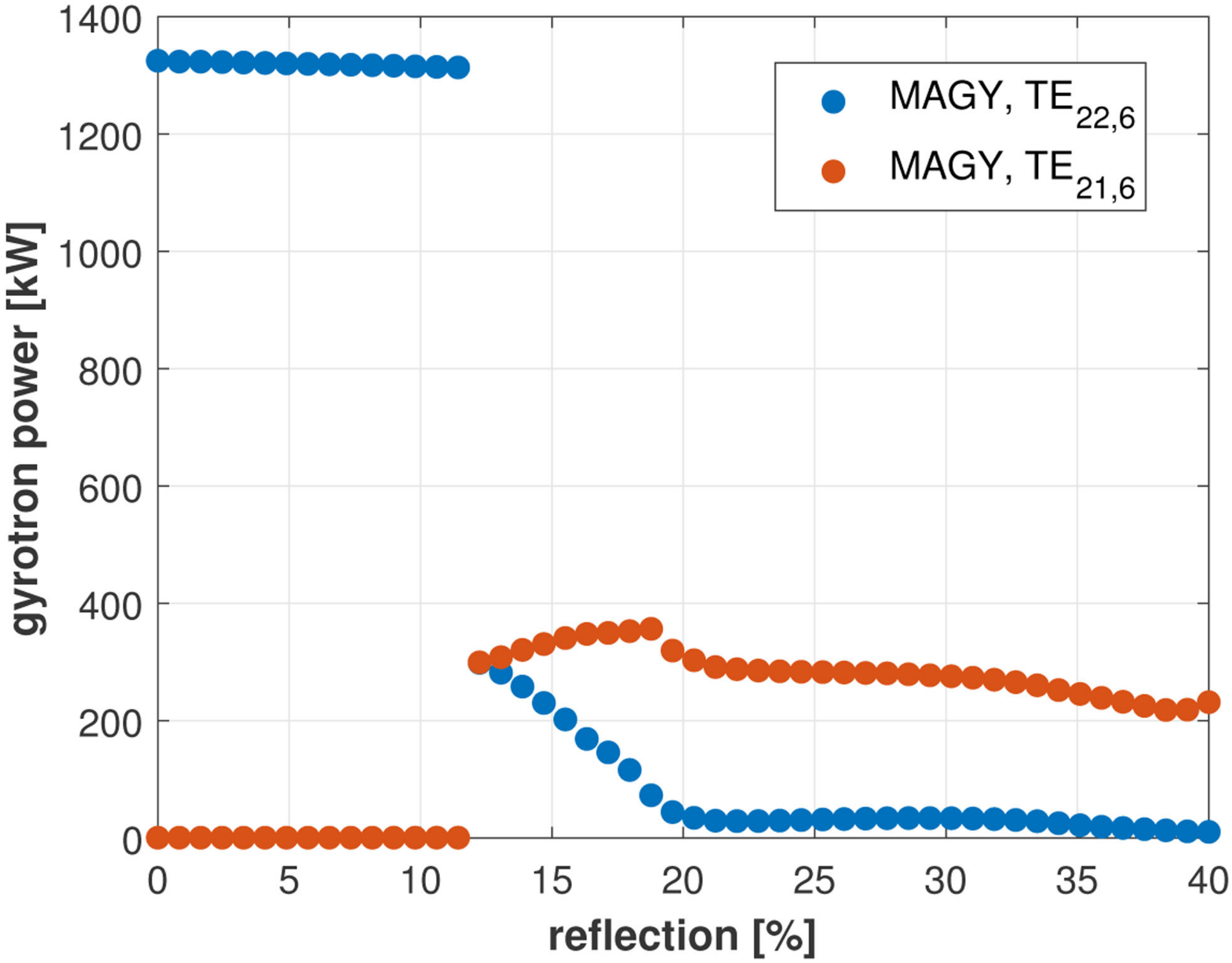

Fig. 9.
High-efficiency operating point. Gyrotron power calculated with MAGY for the two transverse modes $TE_{21,6}$ (in green) and $TE_{22,6}$ (in blue).

Author Manuscript
Author Manuscript
Author Manuscript
Author Manuscript

Table 1

Magnetic field, power and frequency values for the two operating points considered in this study and labeled with the letters A and B in Figure 3.

Operating point	Magnetic field [T]	Output power [kW]	Frequency [GHz]
A: High-efficiency	4.40	940	110.00
B: Stable	4.44	580	110.11

Author Manuscript Author Manuscript Author Manuscript Author Manuscript

Author Manuscript

Author Manuscript

Author Manuscript

Author Manuscript

Table 2

Parameters used for the simulations shown in Fig. 9

Parameter	Value
Transverse modes	$TE_{21,6}$, $TE_{22,6}$, $TE_{23,6}$
Magnetic field	4.40 T
Beam current	39 A
Cathode voltage	96 kV
Pitch angle	1.43